Chemical Engineering Journal 106 (2005) 43–52

Chemical Engineering Journal

www.elsevier.com/locate/cej

Gas flow behavior and residence time distribution in a rough-cut cyclone

Chao Zhongxi[a], Sun Guogang[a], Jinyu Jiao[b], Ying Zheng[b,*], Gong Bing[a], Shi Mingxian[a]

[a] *Department of Chemical Engineering, University of Petroleum, Beijing 102249, PR China*
[b] *Department of Chemical Engineering, University of New Brunswick, 15 Dineen Drive, P.O. Box 4400, Fredrecton, NB, Canada E3B 5A3*

Received 24 January 2004; received in revised form 17 June 2004; accepted 17 June 2004

Abstract

This work studied the gas flow field and oil gas residence time distribution in a rough-cut cyclone. DSM model was applied to simulate the 3-D gas flow field and the simulation results were validated with the experimental data measured by a five-hole probe. A good agreement was obtained. It is shown that a rough-cut cyclone has a gas flow structure different from the one exhibited in a conventional gas cyclone. Reversed flow exists in both the exit tube and dipleg, which can even extend to the main body of cyclone. The reversed flow has a strong impact on the flow structure in a rough-cut cyclone. The residence time distribution of the gas stream was computed using scalar transport equations. The residence time distribution of oil gas in cyclone appears to be a log-normal distribution while a bimodal profile is shown in the reversed flow. A 5–10% increase in the residence time of oil gas is observed, which is attributed to the reversed flow in the exit tube and dipleg. The simulation results also show that reducing the diameter of a dipleg or adding a hopper can accelerate the gas flow movement towards the exit tube as well as reduce the reversed flow in both the exit tube and dipleg. Therefore, the residence time of oil gas is shortened and the higher separation efficiency of a rough-cut cyclone is ensured.

Keywords: Rough-cut cyclone; Simulation; Residence time; Reversed flow

1. Introduction

The gas cyclone that separates catalysts from high temperature oil gas is a key component of fluid catalytic cracking units in refinery plants. Extensive research has been conducted on the flow fields in gas cyclones in order to improve the performance of cyclones. Different measurement techniques such as LDV [1,2], a five-hole probe [3–5], have been employed to measure the flow behaviors in gas cyclones. A rough-cut cyclone is a relatively new type of cyclone, which is different from the conventional ones. Its dipleg and exit tube are both open to the environment and oil gas is allowed to exit this cyclone from either the exit tube or the dipleg. A hopper is unlikely to be installed due to the limited space in fluid catalytic cracking unit (FCCU). The flow characteristics of oil gas in rough-cut cyclones are of great importance for the quick discharging of high temperature oil gas after catalytic cracking reaction in the riser. The distinct configuration of cyclones may introduce different gas flow structure. As a result, it is inappropriate to apply the research results obtained from the conventional cyclones to the rough-cut ones. However, little work has been documented in the literature.

Previously published work has been focused on the pressure drop, cyclone structure and separation efficiency of a gas cyclone. Recently, coking has proven to be the primary problem in FCCU. To reduce coking, it is essential to shorten the gas residence time of products in a FCCU. Therefore, knowledge of the residence time distribution of oil gas in rough-cut cyclones becomes necessary. Hongzhi [6], Wei and Naining [7] studied the residence time distribution using fine particulates tracing technique. Due to the lower velocity of particulates compare to the gas flow, a discrepancy is expected to exist between the experimental results and the

Abbreviations: RTD, residence time distribution; FCCU, fluid catalytic cracking units

* Corresponding author. Fax: +1 506 453 3591.
E-mail address: yzheng@unb.ca (Y. Zheng).

1385-8947/$ – see front matter © 2004 Elsevier B.V. All rights reserved.
doi:10.1016/j.cej.2004.06.014

Nomenclature

a	height of the inlet (mm)
A	transverse area of reversed flow (m^2)
A_r	transverse area of reversed flow in the exit tube (m^2)
$\tilde{A}_r$	simulation result of dimensionless transverse area of reversed flow in the exit tube
$\tilde{A}'_r$	experimental result of dimensionless transverse area of reversed flow in the exit tube
A_0	transverse area of dipleg (m^2)
$\tilde{A}_0$	simulation result of dimensionless transverse area of reversed flow in the dipleg
$\tilde{A}'_0$	experimental result of dimensionless transverse area of reversed flow in the dipleg
b	width of the inlet (mm)
C	concentration of tracing smoke (kg/m^3)
d_r	diameter of exit tube (mm)
d_0	diameter of dipleg (mm)
D_φ	viscous diffusion coefficient
I	turbulence intensity
k	constant
l_r	length of exit tube (mm)
$\tilde{l}_r$	simulation results of dimensionless length of reversed flow in the exit tube
$\tilde{l}'_r$	experimental results of dimensionless length of reversed flow in the exit tube
l	length of reversed flow (mm)
l_0	length of dileg (mm)
$\tilde{l}_0$	simulation results of dimensionless length of reversed flow in the dipleg
$\tilde{l}'_0$	experimental results of dimensionless length of reversed flow in the dipleg
m	constant
n	constant
Q	mass flux entering cyclone through inlet (kg/s)
Q_{up}	simulation result of net mass flux out of exit tube (kg/s)
Q'_{up}	experimental result of net mass flux out of exit tube (kg/s)
Q_{down}	simulation result of net mass flux out of dipleg (kg/s)
Q'_{down}	experimental result of net mass flux out of dipleg (kg/s)
Q_{r1}	mass flux of reversed flow in exit tube (kg/s)
Q_{r2}	mass flux of reversed flow in dipleg (kg/s)
R	radius of cylinder (mm)
r	local radial position (mm)
Sc_t	Schmit number
t	time (s)
t_1	mean residence time of gas from the inlet and out of the exit tube (s)
t_2	mean residence time of gas from the inlet and out of the dipleg (s)
t_3	mean residence time of reversed flow in exit tube (s)
t_4	mean residence time of reversed flow in dipleg (s)
T	integral limit
u_i	gas velocity at the inlet (m/s)
v_t	tangential velocity (m/s)
v_z	radial velocity (m/s)
x	coordinate
y	coordinate
x_0	coordinate x of the center of the inlet
y_0	coordinate y of the center of the inlet

Superscript

$\sim$	dimensionless

Greek letters

λ_1	increase of average residence time because of reversed flow in exit tube
λ_2	increase of average residence time because of reversed flow in dipleg
ε	turbulence dissipation rate (m^2/s^3)
μ	viscosity (Pa s)
μ_t	turbulence viscosity (Pa s)

actual gas residence time. Lede et al. [8] applied the gas tracer technique to study the gas residence time distribution in a high temperature cyclone reactor. Later, van der Lans et al. [9] used helium as a tracer and a fast-response probe to investigate the residence time distribution in a cold swirling flow combustor. The RTD results have been used to verify several CFD models and to derive a chemical reaction engineering model for a mixing process.

Based on numerical simulation and experimental investigation, this work studies the gas flow structure in a rough-cut cyclone, the effect of the diameter of dipleg and the presence of a hopper. The scalar transport equation was used to compute the gas residence time distribution in rough-cut cyclones.

2. Experimental set-up

2.1. Geometry of a rough-cut cyclone

Fig. 1 shows a schematic of a rough-cut cyclone separator. The outer diameter of the cyclone is 500 mm. Air is blown into the inlet of the cyclone after passing a flowmeter that measures gas flow rates. The mean gas inlet velocity (v_i) is 18 m/s. The dipleg and exit tube are both open to the air. In order to study the impact of dipleg diameter and the presence of a hopper on the gas flow behavior and the residence time distribution, four different configurations of rough-cut

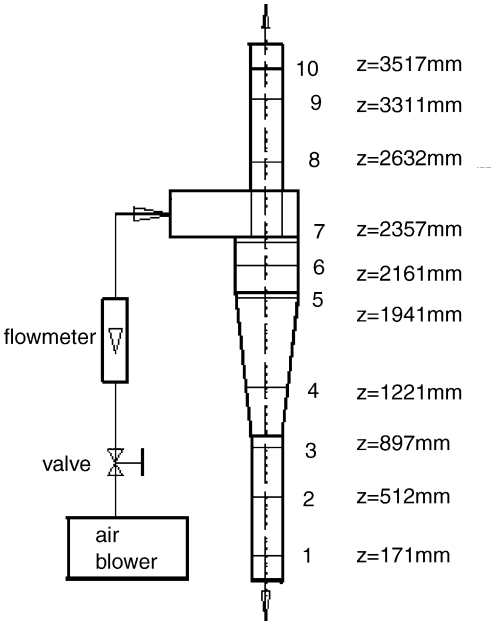

Fig. 1. Schematic diagram of the experimental system.

Table 1
Four different rough-cut cyclones proposed in this study

Cyclone	d_r (mm)	d_0 (mm)	Presence of a hopper
1	240	190	No
2	240	190	Yes
3	240	240	No
4	240	240	Yes

cyclone (shown in Table 1) were investigated. The geometry of the hopper is shown in Fig. 2.

2.2. Measurement techniques

A five-hole probe consisting of an adjustable frame and five pressure transducers was used to measure the axial, radial and tangential velocities of the gas field, as shown in Fig. 3. When the five-hole probe was placed in a flow field, voltage signals obtained through the five pressure transducers were transferred to an amplifier. The magnified voltage signals were acquired through an acquisition system containing a microprocessor and a personal computer. Velocity distribution and static pressure profile can be computed through the software supplied by the manufacturer.

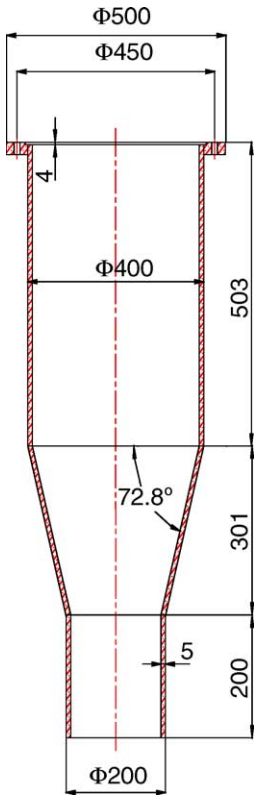

Fig. 2. Schematic of the hopper.

Measurements were conducted at ten different elevations of cyclone (shown in Fig. 1). In each elevation, the five-hole probe moved from the wall of cyclone to its centerline and data were recorded at every 10 mm interval.

3. Numerical simulation

3.1. Flow characteristics in a rough-cut cyclone

Extensive studies have been done on the flow fields of cyclones by means of numerical simulation. There are three stages for the development of a cyclone simulation. Initially, the Navier–Stokes equation was greatly reduced to a

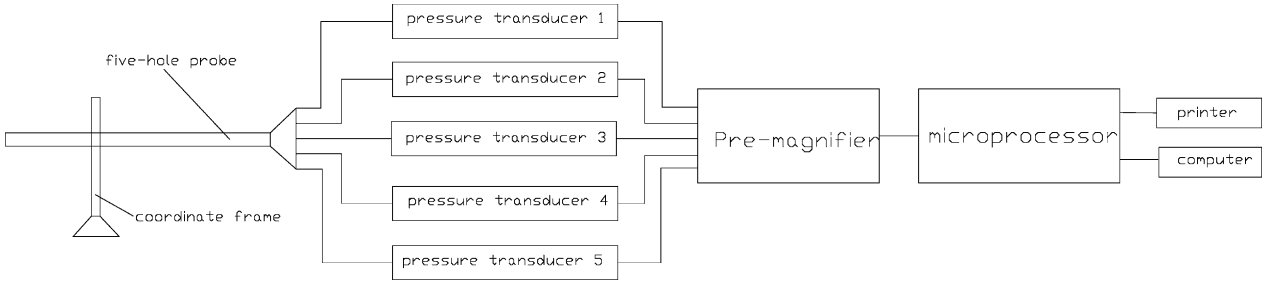

Fig. 3. The measurement system.

semi-empirical correlation for computing tangential velocities, which simplification was on the basis of a large quantity of experimental results. The second stage started with Boyson's work [10]. His principle was that the effect of a 3-D flow was restricted to the tangential inlet zone, and the flow in the main body of a gas cyclone was axisymmetric. With the assumption of axisymmetry, the anisotropic turbulence models: algebraic stress model (ASM) and differential stress model (DSM) were combined to simulate the time-averaged and turbulent flow in cyclones. In his model, the Reynolds' stresses of $\overline{v'w'}$, $\overline{v'^2}$ and $\overline{w'^2}$ were in the differential form whereas Reynolds' stresses of $\overline{u'^2}$, $\overline{u'v'}$ and $\overline{u'w'}$ were in the algebraic form. The tangential velocities computed from this model were well in agreement with experimental results. Fast development in computer technology leads to the third simulation stage. Researchers have successfully applied the k–ε model [1], modified k–ε model [11], the ASM model [12] and DSM model [13] to simulate the flow behaviors in cyclones. It is reported that the anisotropic ASM and DSM models can produce better predictions on a strong swirling flow in cyclones than the isotropic models [12–15]. As a result, the DSM model was selected to study the flow characteristics of a rough-cut cyclone in this work.

(a) Governing equations

The governing equations involve the continuity equations, the momentum equations, the closured stress transport equations and the turbulence dissipation rate equation, which can be expressed as follows:

$$\frac{\partial}{\partial t}(\rho\varphi) + \frac{\partial}{\partial x_j}(\rho u_j \varphi) = \frac{\partial}{\partial x_j}\left(\Gamma_\varphi \frac{\partial \varphi}{\partial x_j}\right) + S_\varphi \quad (1)$$

where φ is a universal variable, Γ_φ is the transport coefficient, S_φ is the source item. The expressions of φ, Γ_φ, S_φ in different equations are listed in Table 2.

(b) Boundary conditions

The boundary condition of the inlet of the rough-cut cyclone can be defined as:

$$u_i = Kv_i\left(1 - \left(\frac{x - x_0}{a}\right)^m\right)\left(1 - \left(\frac{y - y_0}{b}\right)^n\right) \quad (2)$$

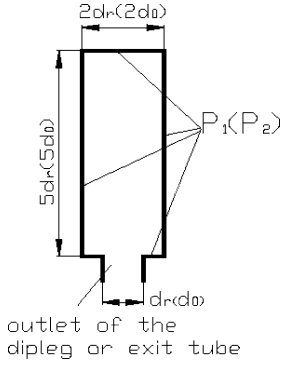

Fig. 4. Boundary conditions of the outlets of the exit tube and dipleg.

Given the turbulence intensity I and hydraulic diameter D_H, the Reynolds stresses $\overline{u_i'u_j'}$ and the turbulence dissipation rate ε at the inlet can be computed.

$$\overline{u_i'u_j'} = k = \frac{3}{2}I^2U^2 \quad (3)$$

$$\varepsilon = \frac{k^{3/2}}{0.3D_H} \quad (4)$$

where $I = 0.037$, $D_H = 224$ mm.

Since the outlets of exit tube and dipleg are open to the FCCU, the outflows are similar to a free swirling jet flow. Analogizing the boundary condition of free swirling jet flow, a larger cylinder can be assumed to attach to the outlets of both the dipleg and the exit tube, whose pressure boundary condition is $P_1 = P_2 = 101325$ Pa (Fig. 4). The Reynolds stresses $\overline{u_i'u_j'}$ and the turbulence dissipation rate ε are treated in a similar way of inlet as presented above.

(c) Wall boundary condition

No slip is assumed at the wall, $\varphi = 0$. The standard wall function provided by CFX5.5 was employed for the fully turbulent layer.

$$u^+ = \frac{U_t}{u_\tau} = \frac{1}{k}\ln(y^+) + C \quad (5)$$

$$y^+ = \frac{\rho \Delta y u_\tau}{\mu} \quad (6)$$

Table 2
Governing equations of DSM model

Equations	φ	Γ_φ	S_φ
Continuity equation	1	0	0
Momentum equation	u_j	μ	$-\frac{\partial p}{\partial x_i} + \frac{\partial}{\partial x_j}\left(\mu\frac{\partial u_j}{\partial x_i} - \frac{2}{3}\delta_{ij}\frac{\partial u_l}{\partial x_l}\right) + \rho g_i$ £ $\frac{\partial}{\partial x_j}(\rho\overline{u_i'u_j'})$
Algebraic stress equation	$\overline{u_i'u_j'}$	$\mu + \frac{2}{3}c_s\rho\frac{k^2}{\varepsilon}$	$P_{ij} + \varepsilon_{ij} + \phi_{ij}$
Turbulence dissipation equation	ε	$\frac{1}{\sigma_{\varepsilon RS}}\left(\mu + \rho C_{\mu RS}\frac{k^2}{\varepsilon}\right)$	$\frac{\varepsilon}{k}(c_{\varepsilon 1}P_{ij} - c_{\varepsilon 2}\rho\varepsilon)$

where $P_{ij} = -\rho\left(\overline{u_i'u_k'}\frac{\partial \overline{u_j}}{\partial x_k} + \overline{u_j'u_k'}\frac{\partial \overline{u_i}}{\partial x_k}\right)$ $\varepsilon_{ij} = -\frac{2}{3}\delta_{ij}\varepsilon\rho$ $\phi_{ij} = \phi_{ij1} + \phi_{ij2}$; $\phi_{ij1} = -\rho\varepsilon\left[C_{s1}a_{ij} + C_{s2}\left(a_{ik}a_{kj} - \frac{1}{3}a_{ij}a_{ji}\delta_{ij}\right)\right]$; $\phi_{ij2} = -C_{r1}Pa_{ij} + C_{r2}\rho k S_{ij} - C_{r3}\rho k S_{ij}(a_{ij}a_{ji})^{1/2} + C_{r4}\rho k\left(a_{ik}S_{jk} + a_{jk}S_{ik} - \frac{2}{3}a_{kl}S_{kl}\delta_{ij}\right) + C_{r5}\rho k(a_{ik}\Omega_{jk} + a_{jk}\Omega_{ik})$; $a_{ij} = \left(\frac{\overline{u_i'u_j'}}{k}\right) - \frac{2}{3}\delta_{ij}$, $k = \frac{\overline{u_i'u_i'}}{2}$; $S_{ij} = \frac{1}{2}\left(\frac{\partial u_i}{\partial x_j} + \frac{\partial u_j}{\partial x_i}\right)$, $S_{ij} = \frac{1}{2}\left(\frac{\partial u_i}{\partial x_j} + \frac{\partial u_j}{\partial x_i}\right)$, $P = \rho\overline{u_i'u_j'}\frac{\partial u_i}{\partial x_j}$.

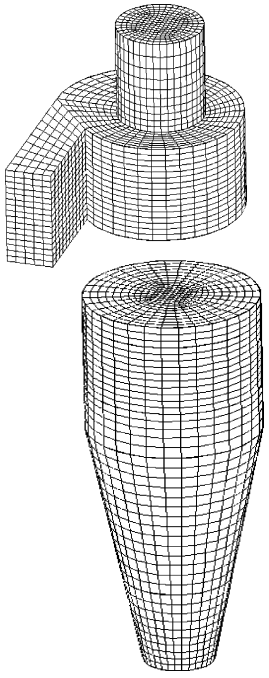

Fig. 5. Meshing of the inlet zone and main body.

$$u_\tau = \left(\frac{\tau_w}{\rho}\right)^{1/2} \tag{7}$$

where u^+ is the velocity close to the cyclone wall; u_τ, the friction velocity; U_t, the known velocity tangent to the wall at a distance of Δy from the wall; y^+, the dimensionless distance from the wall; τ_w, the wall shear stress; k, the Von Karman constant and C is a constant related to wall roughness.

The second order upwind advection scheme was adopted for all equations. Body-fitted technique was used when the grid system was established. In order to generate high quality meshes (Fig. 5), the cyclone was cut into two volumes: the main body and the inlet section that were meshed separately. Then the two independent meshed volumes were combined using the interpolation method.

3.2. Gas residence time distribution

The time that fluid elements have spent in a system is called the residence time of those elements. The residence time distribution is computed by solving the transient scalar transport equation.

The governing equation can be expressed as follows:

$$\frac{\partial \phi}{\partial t} + \nabla\times(U\phi) = \nabla \times \left(\rho D_\phi + \frac{\mu_t}{Sc_t}\right)\nabla \times \left(\frac{\phi}{\rho}\right) + S_\phi \tag{8}$$

Concentration of tracer at the inlet can be expressed as:

$$\phi = C_0 \exp(-\alpha t) \tag{9}$$

The mass flux of tracer at the outlets is a function of time,

$$Q(t) = \int_A V_{out}|C_{out}\mathrm{d}A \tag{10}$$

where A is the area in outlets for outflows and V_{out} denotes the gas velocity at the tracer concentration equal to C_{out}.

There exist reversing zones in both the exit tube and the dipleg of a rough-cut cyclone, that is, a portion of the outflowing gas tends to return back to the exit tube and dipleg. The reversed flow travels down to the bottom of the exit tube and then returns back with upflowing gas. For a rough-cut cyclone, the exit tube and dipleg are both open to environment. The strongly swirling flow produces large pressure gradients, which leads to a lower pressure in the centerline of the exit tube and dipleg. As a result, a gas flow can flow back to the lower pressure zones and the reversed flow occurs.

Four mean residence times of gas flow are defined here. t_1 and t_2 refer to the mean time that a gas travels from the inlet of the cyclone to the outlet of the exit tube and to the outlet of the dipleg, respectively. t_3 and t_4 represent the mean residence time of the reversed flow at the exit tube and the dipleg, respectively.

(a) Computation of t_1 and t_2

After the mass fluxes of gas flow from the exit tube and the dipleg, denoted as $Q_1(t)$ and $Q_2(t)$, are obtained, the mean residence time t_1 and t_2 can be determined.

$$t_1 = \frac{\int_0^T tQ_1(t)\mathrm{d}t}{\int_0^T Q_1(t)\mathrm{d}t} \tag{11}$$

$$t_2 = \frac{\int_0^T tQ_2(t)\mathrm{d}t}{\int_0^T Q_2(t)\mathrm{d}t} \tag{12}$$

(b) Computation of t_3 and t_4

$Q_3(t)$ and $Q_4(t)$ are the mass fluxes of reversed flow at the exit tube and dipleg, respectively. We have,

$$t_3' = \frac{\int_0^T tQ_3(t)\mathrm{d}t}{\int_0^T Q_3(t)\mathrm{d}t} \tag{13}$$

$$t_4' = \frac{\int_0^T tQ_4(t)\mathrm{d}t}{\int_0^T Q_4(t)\mathrm{d}t} \tag{14}$$

The reversing ratios, η_1 and η_2, are defined as $\eta_1 = Q_3(t)/Q_1(t)$ and $\eta_2 = Q_4(t)/Q_2(t)$. Assume the reversing ratios remain constant. Then, the mean residence time of the reversed flow in the exit tube is:

$$t_3 = t_3'(1 + \eta_1 + \eta_1^2 + \ldots) = \frac{t_3'}{1-\eta_1} \tag{15}$$

and the mean residence time of the reversed flow in the dipleg is,

$$t_4 = t_4'(1 + \eta_2 + \eta_2^2 + \cdots) = \frac{t_4'}{1-\eta_2}. \tag{16}$$

The mean residence time of gas in the cyclone is then expressed as,

$$t = \frac{t_1 Q_{up} + t_2 Q_{down}}{Q} + t_3 \frac{Q_{r1}}{Q} + t_4 \frac{Q_{r2}}{Q} \quad (17)$$

The gas residence time increase due to the reversed flow in the exit tube and dipleg is:

$$\lambda_1 = \frac{t_3(Q_{r1}/Q)}{(t_1 Q_{up} + t_2 Q_{down})/Q} \quad (18)$$

$$\lambda_2 = t_4 \frac{Q_{r2}/Q}{(t_1 Q_{up} + t_2 Q_{down})/Q} \quad (19)$$

4. Results and discussion

4.1. Experimental verification

The simulation results of tangential and axial velocities as well as the static pressure distribution are compared with the experimental results in Figs. 6–8. Good agreements are obtained, which suggests that the DSM model (see Table 3) is effective in predicting the characteristic of gas flow in rough-cut cyclones. Since the radial velocities (mostly on the order of 10^{-1} m/s) are out of test range of the five-hole probe, the measurement results are not in good agreement with the simulation results, and thus the comparison was not given here.

4.2. Comparison of a rough-cut cyclone and a conventional cyclone

Figs. 9 and 10 show the comparisons of simulation predictions of flow fields between a rough-cut cyclone and a conventional one. It is seen that unlike a conventional cyclone, there exists a reversed flow in the dipleg and exit tube in a rough-cut cyclone. The tangential velocity distribution in the main body of a rough-cut cyclone appears to be similar to that in a conventional cyclone. The external quasi-free vortex, the internal quasi-forced vortex and the external swirling flow dominate the entire flow field. The maximum tangential velocity presents at the intersection of the two swirling flows and can be expressed as $\tilde{v}_t = C\tilde{r}^n$. The axial velocities in the solid separation region of rough-cut cyclone are quite

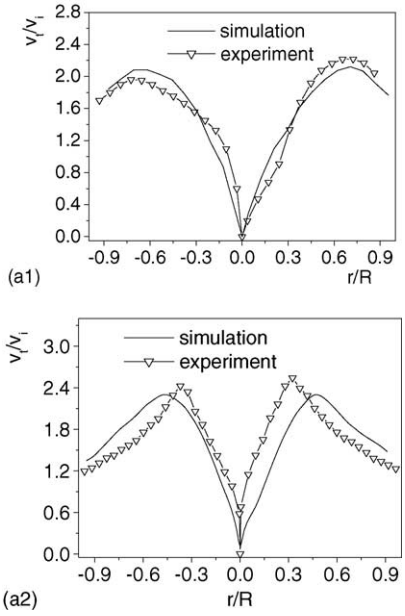

Fig. 6. Comparison of the tangential velocities between simulation results and experimental data (a1) $z = 171$ mm; (a2) $z = 2161$ mm.

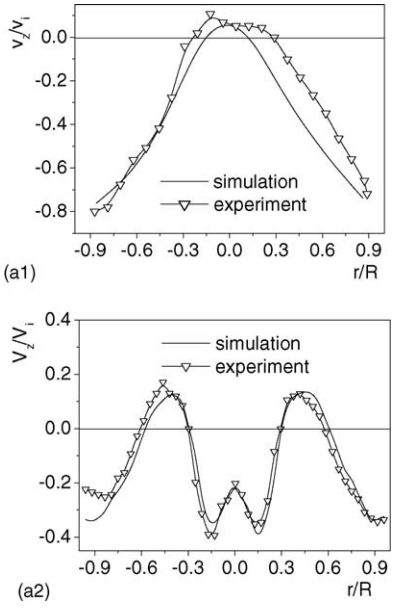

Fig. 7. Comparison of the vertical velocities between simulation results and experimental data (a1) $z = 171$ mm; (a2) $z = 2161$ mm.

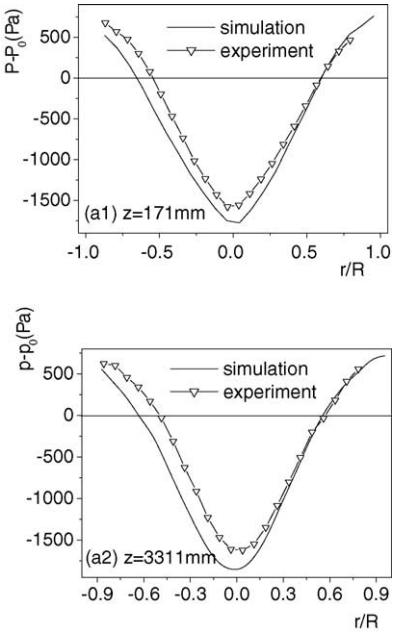

Fig. 8. Comparison of the static pressure between simulation results and experimental data (a1) $z = 171$ mm; (a2) $z = 2161$ mm.

Table 3
Constants shown in the DSM model

$c_{\mu RS}$	0.115
$\sigma_{\varepsilon RS}$	1.10
c_s	0.22
$c_{\varepsilon 1}$	1.45
$c_{\varepsilon 2}$	1.9
c_{s1}	1.8
c_{s2}	0.0
c_{r1}	0.0
c_{r2}	0.8
c_{r3}	0.0
c_{r4}	0.6
c_{r5}	0.6

different from that in conventional cyclone separators (as shown in Figs. 11 and 12). The distribution can be categorized into three characteristic zones in axial direction. In the upper zone, due to the influence of reversed flow in the exit tube, the local axial velocity near the wall and in the centerline appear to be downward but upward in the middle area. In the mid-zone, the downward axial velocity occurs only near to the wall. In the lower zone, the downward axial velocity dominates the entire cross-sectional area. As a result of the existence of reversed flow, the axial velocity behaves

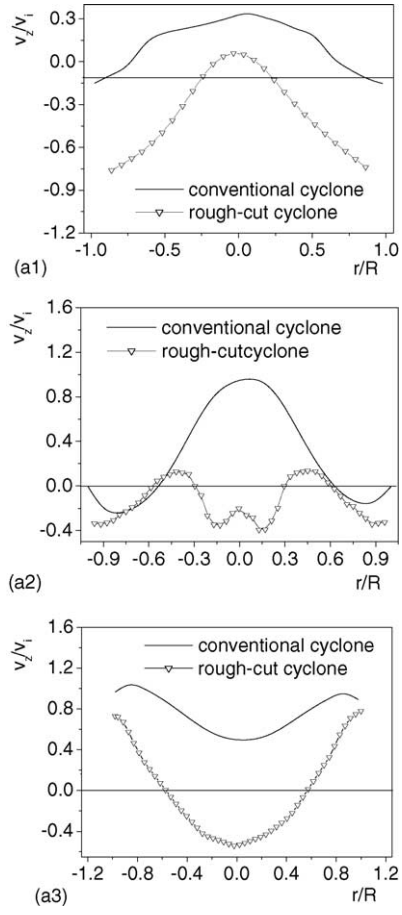

Fig. 9. Comparisons of the axial velocities in the rough-cut cyclone and in a conventional one (a1) $z = 171$ mm; (a2) $z = 2161$ mm; (a3) $z = 3311$ mm.

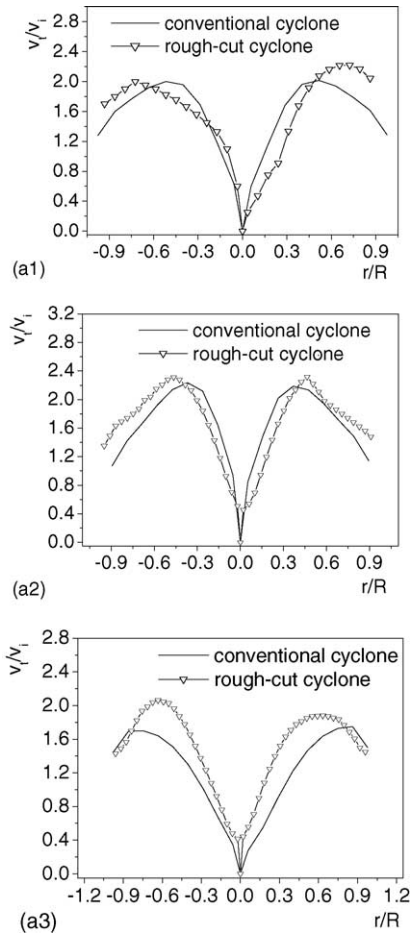

Fig. 10. Comparisons of the tangential velocities in the rough-cut cyclone and in a conventional one (a1) $z = 171$ mm; (a2) $z = 2161$ mm; (a3) $z = 3311$ mm.

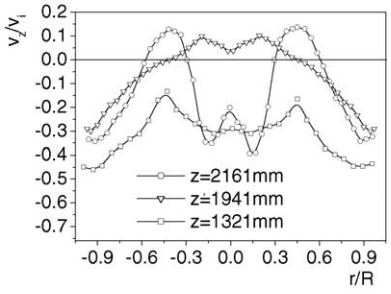

Fig. 11. Axial velocities in the separation space in a rough-cut cyclone.

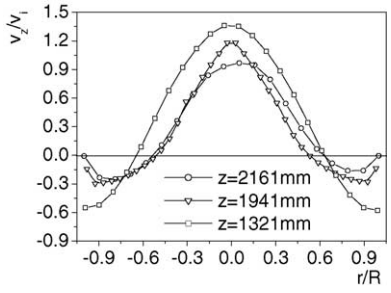

Fig. 12. Axial velocities in the separation space in a conventional cyclone.

differently in the exit tube: the velocity is upward near the wall but downward in the center. Similar to conventional cyclones, the tangential velocity in the rough-cut cyclone can be categorized into the external and internal flow. The boundary between the two flows is approximately at 1/4 of the radius from the wall of the exit tube. The internal one dominates the flow filed. In the dipleg of rough-cut cyclone, the axial velocity is always downward at the top end while in the lower end, the axial velocity is split into two regions: downward near the wall and upward in the center region. The flow characteristics of tangential velocity in the dipleg are similar to those in the exit tube.

4.3. Reversing zones in the exit tube and dipleg

Both of the experimental and simulation results reveal that the reversed flow in the exit tube and dipleg has a significant effect on the flow field in rough-cut cyclones. Two dimensionless parameters, the relative height and the relative transverse area of reversed flow are defined as follows:

$$\tilde{l}_\mathrm{r} = \frac{l}{l_\mathrm{r}} \left(\tilde{l}_0 = \frac{l}{l_0} \right), \tag{20}$$

$$\tilde{A}_\mathrm{r} = \frac{A}{A_\mathrm{r}} \left(\tilde{A}_0 = \frac{A}{A_0} \right) \tag{21}$$

Table 4 lists the experimental and simulation results of the relative height and relative transverse area of the four cyclones that are given in Table 1. Note that the reversed zones occupy large areas in both the exit tube and the dipleg. In the vertical direction of the exit tube, the reversed flow zone can extend up to 160 mm above the particle separation space and take up about 46% of the cross-sectional area of the exit tube. The maximum relative length of the reversed flow in the dipleg is 0.54, and the maximum relative transverse area is 0.43. Undoubtedly, the reversed flow has a great negative impact on the performance of rough-cut cyclones. The reversed flow in the exit tube increases resistance to the upflow gas, which resistance enforces a large amount of oil gas associated with catalysts to travel down to the dipleg. For example, about 71.1% of the total mass flux of Cyclone 3 flows out of the rough-cut cyclone through the dipleg. However, the reversed flow in the dipleg has the same function—to increase resistance to the outflowing stream. Apparently, the separation efficiency of the cyclone suffers due to the reversed flow. Furthermore, the reversed flow lengthens the mean residence time of oil gas, which enhances the probability of coking.

Table 4
Dimensionless parameters of the reversed flow in the exit tube and dipleg

Cyclone	$\tilde{l}_\mathrm{r}$	$\tilde{l}'_\mathrm{r}$	$\tilde{l}_0$	$\tilde{l}'_0$	$\tilde{A}_\mathrm{r}$	$\tilde{A}'_\mathrm{r}$	$\tilde{A}_0$	$\tilde{A}'_0$
1	0.186	0.15	0.098	0.087	0.18	0.21	0.114	0.09
2	0.014	0.02	0.019	0.014	0.037	0.05	0.015	0.02
3	1.16	1.24	0.54	0.43	0.46	0.51	0.43	0.37
4	0.041	0.05	0.046	0.037	0.088	0.10	0.047	0.07

Experimental and simulation results shown in Table 4 illustrate that the presence of a hopper and the decrease of the diameter of the dipleg can significantly reduce the reversed flow. Compared to Cyclone 3, Cyclone 2 has added a hopper and reduced the diameter of dipleg by 21%, which modifications lead to a 98% decrease in the relative length of reversed flow and a 96% decrease in the relative cross-sectional area of the exit tube. The reversed flow in the dipleg of Cyclone 2 is mostly removed. As a result, a noticeable increase can be observed in the mass flux of gas flow exiting from the exit tube. Cyclone 1 has a similar configuration to Cyclone 3 except for a smaller dipleg, as shown in Table 1. The gas flow discharging from the exit tube of Cyclone 1 has significantly enlarged in comparison with Cyclone 3. Apparently, the variations can improve the gas–solid separation efficiency and decrease the high temperature oil gas residence time. Therefore, a small dipleg and the addition of a hopper are essential for a rough-cut cyclone to improve the gas–solid efficiency and reduce the oil gas residence time if the space in a FCCU allows it.

4.4. Residence time distribution

The typical simulation results of gas residence distribution obtained in rough-cut cyclones are shown in Figs. 13–15. Fig. 13 shows the results of gas residence time distribution for the case that the tracer was introduced at the inlet and the tracer concentration was monitored at the outlets of exit tube and dipleg. The RTD profile follows a log-normal distribution. The two RTD profiles indicate that the gas flow entering the inlet of the rough-cut cyclone mainly flows through the dipleg, which is in good agreement with the partition of mass flux between the exit tube and dipleg (shown in Table 5). The mass flux of tracer flowing through the exit tube reaches its

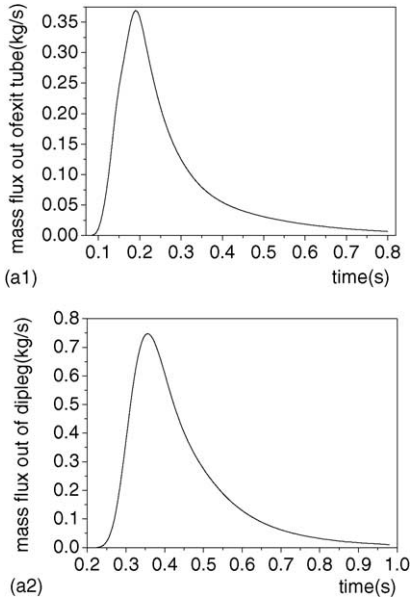

Fig. 13. Residence time distribution of gas. (a1) From the inlet to the exit tube; (a2) from the inlet to the dipleg.

Table 5
Influence of the dipleg diameter and the presence of a hopper on mass flux distribution

Cyclone	Q_{up}/Q	Q'_{up}/Q	Q_{down}/Q	Q'_{down}/Q
1	0.786	0.816	0.214	0.184
2	0.907	0.919	0.093	0.081
3	0.289	0.322	0.711	0.678
4	0.634	0.713	0.366	0.287

maximum at 0.2 s whereas the mass flux of down-flowing tracer through the dipleg attains its peak at 0.34 s. It indicates that it takes a longer residence time for oil gas to discharge through the dipleg than the exit tube. When the residence time of gas oil increases, more coke tends to be generated.

Fig. 14 shows a bimodal profile for the residence time distribution when both the introduction of tracer and the monitor of tracer concentration take place at the outlets of the exit tube. The maximum mass flux is shown at 0.065 s, and the second peak occurs at 0.34 s. This distribution is determined by the characteristics of reversed flow. The vector profile (shown in Fig. 16(a1)) and the stream line (shown in Fig. 17) reveal that the presence of reversed flow can strongly affect the flow structure in the particle separation area. With an outward vector in the radial velocity, a portion of the reversed flow joins the up-flowing zone, which forms the first peak. The rest of the reversed flow keeps moving downwards until it reaches the lower zone of the exit tube and goes up towards the outlet of the exit tube. This reversed flow contributes to the second peak. Fig. 15 shows the gas residence time distribution when tracer was introduced to the reversed flow zone at the outlet of the dipleg, and tracer concentration was recorded at the same place. The radial velocity of reversed flow in the dipleg is outward as shown in Fig. 16 (a2). Following the same reasoning, two peaks of tracer concentration are expected for RTD of the reversed flow in the dipleg: one peak at 0.02 s and the other at 0.08 s as shown in Fig. 15.

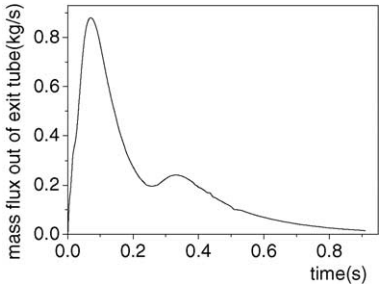

Fig. 14. Gas residence time distribution of the reversed flow in the exit tube.

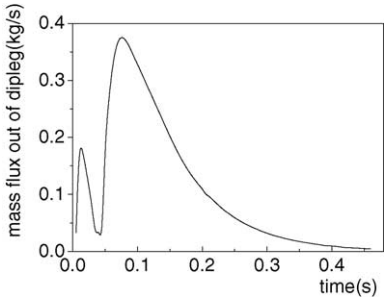

Fig. 15. Gas residence time distribution of the reversed flow in the dipleg.

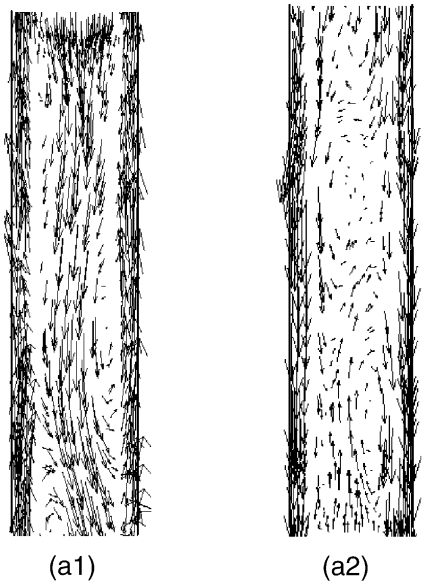

Fig. 16. Velocity vector profile (a1) in the exit tube; (a2) in the dipleg.

4.5. *Effects of dipleg diameter and the presence of a hopper*

Mass flux distribution between the exit tube and the dipleg has a strong impact on the gas residence time in rough-cut cyclones. As discussed in Section 4.4, the mean gas residence time reduces with decreasing the gas flowrate ratio of the dipleg to the exit tube. This work has studied the influence of dipleg diameter and presence of a hopper on the exit tube/dipleg mass flux distribution. The simulation and

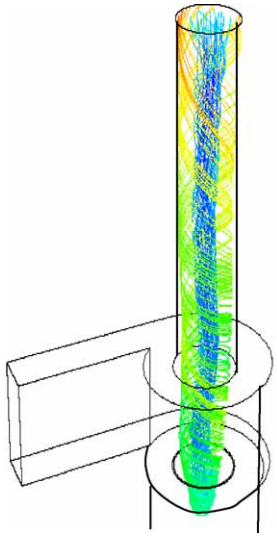

Fig. 17. Stream line in the exit tube.

Table 6
Averaged gas residence time for different rough-cut cyclones

Cyclone	t_1 (s)	t_2 (s)	t_3 (s)	t_4 (s)	t (s)	λ_1(%)	λ_2 (%)
1	0.217	0.478	0.146	0.011	0.288	5.91	0.007
2	0.196	0.513	0.114	0.0	0.241	6.90	0.0
3	0.27	0.439	0.317	0.141	0.423	9.57	1.9
4	0.241	0.467	0.186	0.017	0.345	6.17	0.02

experimental results are shown in Table 5. It is seen that the mass flux distribution between the exit tube and dipleg is very sensitive to variations in the diameter of the dipleg and the presence of a hopper. Either decreasing the diameter of the dipleg or adding a hopper to the rough-cut cyclone can increase the mass flux of gas through the exit tube.

Table 6 shows the simulation results of mean gas residence time in different rough-cut cyclones. With addition of a hopper and reduction of dipleg diameter by 21%, a 43% decrease in gas residence time is gained in Cyclone 2 in comparison with Cyclone 3. It may be attributed to the following reasons: first, decreasing the dipleg diameter or adding a hopper can increase the resistance at the dipleg side and thus most of gas goes upward and releases from the exit tube; second, a large amount of gas goes upwards resulting in the reduction of reversed flow in the exit tube. The reversed flow is present only in the upper zone of the exit tube. The gas flow in the upper zone of the particle separation area becomes stagnant.

5. Conclusions

(1) DSM model can effectively predict flow structure of rough-cut cyclones if suitable meshing system, boundary conditions etc. are selected.
(2) The flow field in a rough-cut cyclone is very different from that in a conventional one, which results from the differences of the outlet boundary conditions of the exit tube and the dipleg.
(3) Decreasing dipleg diameter and adding a hopper can greatly reduce reversed flow and increase the mass flux through the exit tube. This finding is useful in improving the oil-catalyst separation efficiency and in reducing the high temperature oil gas residence time in rough-cut cyclones.
(4) The RTD simulation reveals that a log-normal distribution is obtained for the major gas flow while a bimodal profile represents the residence time distribution of reversed flow in the dipleg and exit tube.
(5) Oil gas residence time in a rough-cut cyclone is generally shorter than 0.5 s. It can be reduced to less than 0.25 s by decreasing dipleg diameter or adding a hopper.

References

[1] L.X. Zhou, S.L. Soo, Gas–solid flow and collection of solids in a cyclone separator, Powder Technol. 63 (1990) 45–53.
[2] A.J. Hoekstra, J.J. Derksen, H.E.A. Van Den Akker, An experimental and numerical study of turbulent swirling flow in gas cyclones, Chem. Eng. Sci. 54 (1999) 2055–2065.
[3] J. Zhongli, S. Mingxian, Study of flow characteristics of cyclone separators with a spiral inlet, J. Petrol. Univ. 16 (1) (1992) 47–53, scientific version.
[4] T. Yanhui, J. Zhongli, S. Mingxian, Study of flow characteristics of PV cyclone separators, J. Petrol. Univ. 16 (1) (1992) 54–59, scientific version.
[5] W. Yaodong, Y. Hui, S. Mingxian, Study on flow field in the annular space of a cyclone separator with a volute inlet, Petrol. Process. Petrochem. 31 (11) (2000) 46–50.
[6] G. Hongzhi, Numerical simulation of transfer process, Metall. Ind. Press (1998) 258–263.
[7] L. Wei, W. Naining, 3-Dimensional simulation of two phase flow in cyclone separators, Power Eng. 19 (1) (1999) 72–80.
[8] J. Lede, H.Z. et, J. Villermaux, Le Cyclone Reacteur Partie I: Mesure Directe de la Distribution des Temps de Sejour de la Phase Gazeuse-Lois d'Extrapolation, Chem. Eng. J. 42 (1989) 37–56.
[9] R.P. van der Lans, P. Glarborg, K. Dam-Johansen, P.S. Larsen, Residence time distribution in a cold, confined swirl flow: implications for chemical engineering combustion modeling, Chem. Eng. Sci. 52 (1997) 2743–2756.
[10] F. Boyson, et al., Experimental and theoretical studies of cyclone separators, Aerodynamics, I. Chem. Eng. Symp. Ser. (1982).
[11] J. Hua, 3-Dimensional simulation of flow in cyclone separators with fitted body, Ph.D. thesis, Petroleum University, Beijing, 1996.
[12] Zhangjian, S. Nieh, Simulation of gas–solid two phase flow in a confined strong swirling flow, Res. Dev. Hydrodyn. 15 (4) (1999) 467–475.
[13] A.J. Hoekstra, E. Van Vliet, J.J. Derksen, H.E.A. Van Den Akker, Advances in turbulence VII, in: Vortex Core Precession in a Gas Cyclone, Kluwer Academic Publishers, Netherlands, 1998, pp. 289–292.
[14] Z. Lixing, Dynamics of Multiphase Turbulent Reacting Fluid Flows, National Defense Industry Press, 2002, pp. 78–101.
[15] Z. Jianxing, Numerical Simulation of Combustion, Scientific Technology Press, 2002, pp. 51–80.